IOP Conference Series: Materials
Science and Engineering

PAPER • OPEN ACCESS

Assembly Trajectory Planning of Space Telescope Sub-mirror Module Based on Time Optimal Control

To cite this article: Hao Ziran *et al* 2018 *IOP Conf. Ser.: Mater. Sci. Eng.* **439** 032077

Assembly Trajectory Planning of Space Telescope Sub-mirror Module Based on Time Optimal Control

Hao Ziran, Jiang Zainan*, Li Chongyang, Yang Fan

(State Key Laboratory of Robotics and Systems,Harbin Institute of Technology Harbin 150001 China)

*Cooresponding author, jiangzainan@hit.edu.cn.

Abstract. The space telescope stands for the highest level of a nation's aerospace industry, with its manufacturing and launch remaining a worldwide conundrum. The concept of modularized space telescope is proposed herein, the main structure of the sub-mirror module is designed briefly and the assembly scheme of the main telescope is also provided. Besides, the kinematic equation and working conditions of the space robotic arm used for assembly are given, with the cubic B-spline curves formulating the joint space trajectory. Then, with minimizing the moving time as the objective of optimization, displacement, speed and acceleration as the constraint conditions, a mathematical model for time-optimal trajectory planning is established and the genetic algorithm is used to work out solutions. The emulation result shows that the joint space trajectory of the robotic arm obtained on the premise that all the restraint conditions are met can minimize the robotic arm's moving time.

1. Introduction

Compared with ground-based telescopes, space telescopes have such advantages such as not subjecting to interference from the atmosphere and the ability to capture high-resolution images. In particular, space telescopes with large calibers and high surface accuracy can observe more intricate structures of objects within higher frequency bands, so it is of great significance for exploration in the unknown space.

Since the launch of the Hubble Space Telescope, America has nearly monopolized the manufacturing, launch and maintenance of space telescopes. So far, America has developed many concepts and models of new large-caliber space telescopes, such as the 20m-caliber Next-Next Generation Space Telescope (NNGST) and the 30m-caliber Thirty Meter Space Telescope (TMST). Yet, as the traditional holistic main telescope requires larger launch space and launch load, these are still concepts that haven't been realized. To meet the requirements, the 6.5m-caliber James Webb Space Telescope (JWST) newly developed by America adopts the solution of folded launch and on-orbit unfolding to reduce the bulk of the telescope during the launch. However, after folding, the JWST (6.5m-caliber) is still sized at 4.47m, which is close to the effective load limit size of the rocket (4.5m); besides, the larger the telescope's caliber is, the larger the launch load is, which means this method is still subject to limitation of the rocket's maximum launch load. Moreover, development of a large-caliber space telescope with the caliber larger than 7 meters calls for better techniques in processing large-caliber reflector as well as better ability in ground-based installation, adjustment, test and experiment.

In fact, both traditional holistic and unfolded space telescope takes the telescope as an integrated whole. But the idea of designing large-caliber telescopes proposed herein is to launch the modularized

IOP Conf. Series: Materials Science and Engineering **439** (2018) 032077 doi:10.1088/1757-899X/439/3/032077

telescope parts into the space and then to complete assembly with the ring-shaped mobile devices and the robotic arm attached to the telescope. The space telescope consists of the primary mirror, secondary mirrors and the sunshield, among which the primary mirror is the main component. How to install and assemble the primary mirror remains the most important and difficult task in the whole assembly process. With the assembly scheme for the sub-mirror module in the space telescope's primary-mirror system provided herein, this paper works out the model of the space robotic arm and the makes kinematic analysis on its workspace. Then, making use of the uniform cubic B-spline curves used in the joint space, this paper works out the joint trajectory of the space robotic arm with continuous speed and acceleration. On this basis, a mathematical model for time-optimal trajectory planning is established and the genetic algorithm is used to find solutions.

2. Sub-mirror Module and Assembly Scheme

2.1. Sub-Mirror Module

Given the space environment, launch requirements, properties of the robotic arm and the post-assembly structural features, the concept of modularized large-caliber space telescope is proposed herein. After the launch vehicle enters the orbit, the space robotic arm draws the modularized components from the capsule and, through automatic or remote control, complete the assembly on orbit. The space telescope module consists of the sub-mirror module, the secondary mirror module, the secondary-mirror truss module, the core module and the sunshield, as is shown in Fig. 1 below.

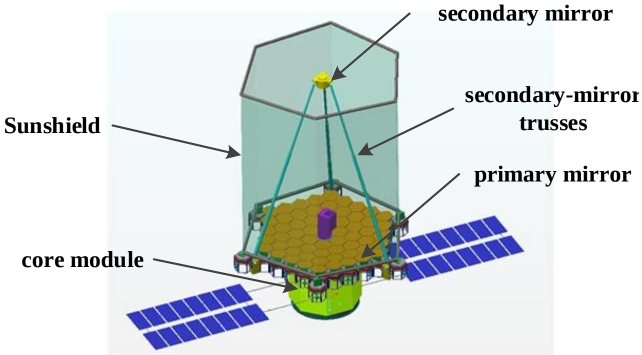

Figure 1. components of space telescope system

As the main part of the primary-mirror system, the secondary mirror module is specifically researched and designed herein. To protect the primary-mirror system from outside interferences and ensure its safe and stable operations, the holistic framework shall be constructed with high levels of rigidity, strength and stability.

The primary-mirror array comprises the sub-mirrors, active optical adjusting components, sub-mirror supporting trusses, an electric cabinet, a target adapter and inter-modular locating & locking elements.

To ensure the structure's rigidity and strength and meet the light weight requirement, all-carbon fiber structure is to be used to design the sub-mirror supporting trusses. The structure of the sub-mirrors is shown in Fig. 2.

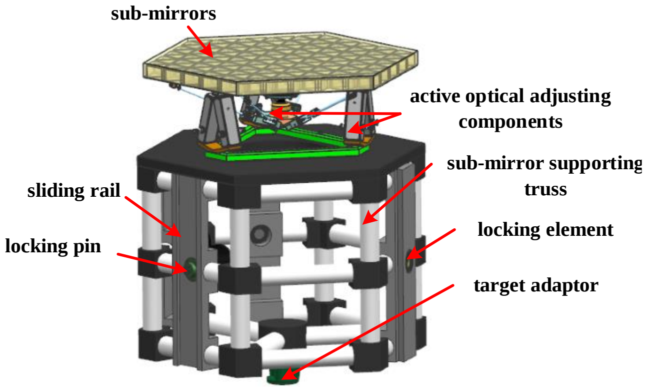

Figure 2. sub-mirror module

Different from assembly schemes which set the trusses before install the mirror, this scheme integrates the highly-modularized trusses with the optical components, and when assembling the primary-mirror system with the mirror module, it completes the assembly of the trusses and the mirror.

2.2. Assembly Scheme

The telescope consists of 60 sub-mirror modules which are placed on four layers, with 6 on the first layer, 12 on the second, 18 on the third and 24 on the fourth. To ensure rigidity, strength and stability of the telescope during assembly, layered-assembly is adopted, that is, assembling the parts from the first layer to the fourth layer in sequence and when assembly of the sub-mirror modules on one layer is finished, it moves to the next layer. During the assembly, two different sub-mirror modules are used, as shown in Fig. 3.

(a) sub-mirror module I (b) sub-mirror module II

Figure3. Basic Modules

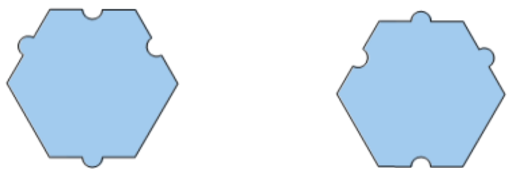

(a) sub-mirror module I (b) sub-mirror module II

Figure 4. Simplified Basic Modules

The regular hexagon stands for the holistic structure, the convex for the assisting sliding rail and the concave for the main sliding rail. The modules can be simplified as Fig. 4.

As is shown in the figures above, except the top part of the large hexagon on the third layer which uses the twelve Modules II, all other parts use Module I.

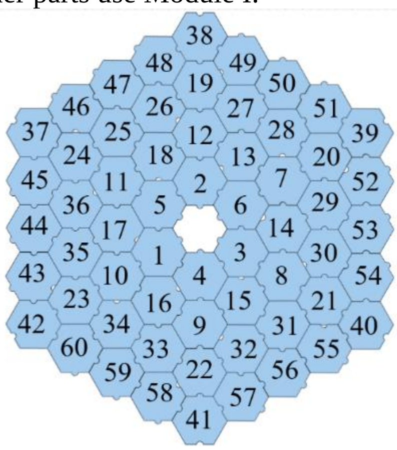

Figure 5. primary-mirror system assembly order

3. Space Robotic Arm Model

3.1. Space Robotic Arm

To fulfill on-orbit assembly and maintenance, the robotic arm is used in assembly. The assembly system consists of a ring-shaped mobile base, a 9-degree-of-freedom space robotic arm, a central controller, two end actuators, two dual-channel cameras, as shown in Fig. 9. The arm is first folded into the flank of the space telescope's resource cabin and is then installed onto the ring-shaped mobile base to move along the circle, hence realizing 360-degree coverage of the workspace.

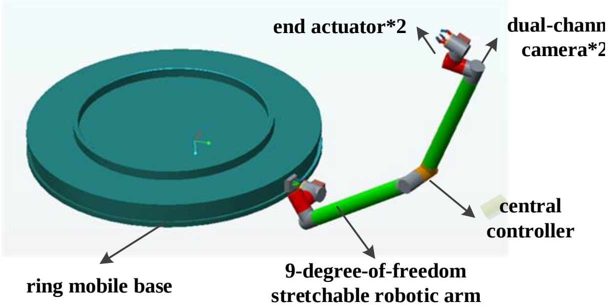

Figure 6. space robotic arm model

3.2. Kinematic Model

With the optimized D-H modelling method, the coordinates are built as shown in Fig. 7. Table 1 presents the corresponding D-H parameters.

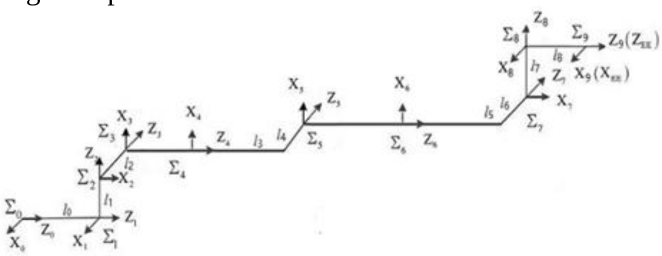

Figure 7. 9-degree-of-freedom redundant space robotic arm D-H coordinates

Table 1. D-H parameters of the 9-dgree-of-freedom redundant space robotic arm

i	θ_i(deg)	d_i(mm)	a_{i-1}(mm)	α_{i-1}(deg)
1	θ_1	700	0	0
2	θ_2	430	0	90
3	θ_3	430	0	-90
4	0	l_3	0	-90
5	θ_5	387	0	90
6	0	l_5	0	-90
7	θ_7	430	0	90
8	θ_8	430	0	90
9	θ_9	700	0	-90

The homogeneous transformation matrix of the end coordinates against the base coordinates, i.e. the forward kinematic model of the robotic arm is:

$$ {}^{0}_{7}T = {}^{0}_{1}T\,{}^{1}_{2}T\,{}^{2}_{3}T\,{}^{3}_{4}T\,{}^{4}_{5}T\,{}^{5}_{6}T\,{}^{6}_{7}T\,{}^{7}_{8}T\,{}^{8}_{9}T \qquad (1)$$

In this paper, the damped least squares method and the gradient projection method are used to work out the inverse kinematic model:

$$\dot{q} = J^{*}\dot{p} + K(I - J^{+}J)\nabla H \qquad (2)$$

IOP Conf. Series: Materials Science and Engineering **439** (2018) 032077 doi:10.1088/1757-899X/439/3/032077

where J stands for transformation matrix between the arm's end speed $\dot{p}$ and the joint speed $\dot{q}$, which is also called the Jacobian matrix; $J^{+} = J^{\mathrm{T}}(JJ^{\mathrm{T}})^{-1}$ stands for the pseudo-inverse value of the Jacobian matrix; H for the gradient of the performance index; K for the optimization coefficient.

3.3. Workspace

Relatively large workspace is needed in the first assembly stage of the robotic arm, but the reachable workspace refers to the largest workspace that the arm can reach. Herein, the Monte Carlo method[] is used to calculate the reachable access.

In fact, fixing the arm's base onto the ring-shaped mobile device is equivalent to giving an extra degree of freedom to the arm. According to the relative position of the robotic arm and the pre-assembled sub-mirror modules in the coordinate system, the arm's reachable workspace when the arm stretches to the maximum and minimum length is drawn, as is shown in Fig. 8.

As can be seen, all the pre-assembling points are within the arm's reachable workspace, that is to say, from the first to the fourth layer, the robotic arm can fulfill different assembly tasks by stretching the length of the arm.

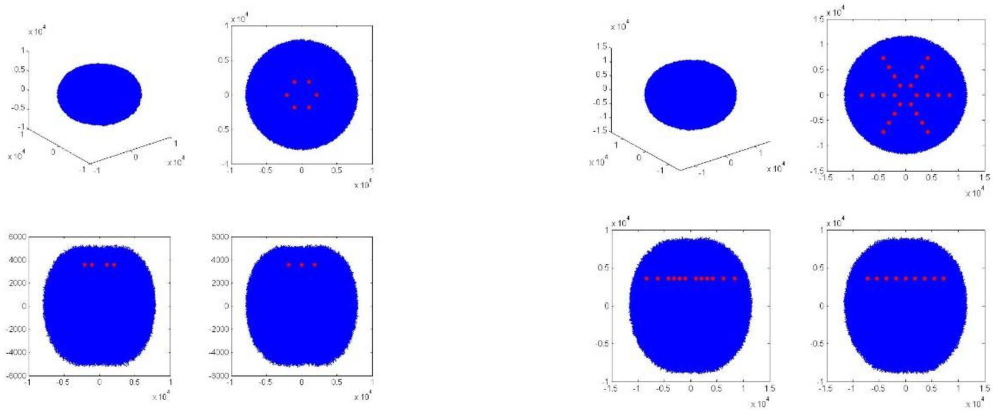

Figure 8. Workspace when the arm stretches between the minimum length and the maximum length

4. Time-Optimal Trajectory Planning

4.1. Uniform Cubic B-Spline Trajectory Planning in Joint Space

Expression of cubic B-spline is :

$$P_j(u) = \sum_{i=0}^{3} d_{j+i} N_{i,3}(u) \tag{3}$$

where

$$\begin{cases} N_{0,3}(u) = (-u^3 + 3u^2 - 3u + 1)/6 \\ N_{1,3}(u) = (3u^3 - 6u^2 + 4)/6 \\ N_{2,3}(u) = (-3u^3 + 3u^2 + 3u + 1)/6 \\ N_{3,3}(u) = u^3/6 \end{cases} \tag{4}$$

$P_j (j = 0,1,...,n-2)$ is the end moving path point, or the data point; $d_{j+i} (j+i = 0,1,...,n+1)$ refers to the control vertex; $N_{i,3}(u)$ stands for the primary function of the uniform cubic B-spline, and $u \in [0,1]$ is the parameter.

To put (4) into (3) to matrix the equation and the result is:

$$P_j(u) = \frac{1}{6}[u^3 \ u^2 \ u \ 1]\begin{bmatrix} -1 & 3 & -3 & 1 \\ 3 & -6 & 3 & 0 \\ -3 & 0 & 3 & 0 \\ 1 & 4 & 1 & 0 \end{bmatrix}\begin{bmatrix} d_j \\ d_{j+1} \\ d_{j+2} \\ d_{j+3} \end{bmatrix} \tag{5}$$

Analysis of (5) leads to:

$$P_j(u) = R_0 + R_1 u + R_2 u^2 + R_3 u^3 \tag{6}$$

where

$$\begin{cases} R_0 = (d_j + 4d_{j+1} + d_{j+2})/6 \\ R_1 = (-d_j + d_{j+2})/2 \\ R_2 = (d_j - 2d_{j+1} + d_{j+2})/2 \\ R_3 = (-d_j + 3d_{j+1} - 3d_{j+2} + d_{j+1})/6 \end{cases} \tag{7}$$

When planning the trajectory, the value of the data point P_j is given to work out the value of the control vertex d_{j+i}; when $u = 0$, the value of P_j is:

$$P_j = \frac{1}{6}\left(d_j + 4d_{j+1} + d_{j+2}\right) \tag{8}$$

where the number of constraint conditions is $n-1$, while that of the control vertex is $n+1$. To facilitate calculation, two extra conditions are added :

$$d_0 = d_1,\ d_{n-1} = d_n \tag{9}$$

With (8) and (9), the previous control vertex can be worked out: $d_i (i = 0,1,...,n)$.

4.2. Mathematical Model of Time-Optimal Trajectory Planning

(1) Target Function

Every joint of the space robotic arm is given $m+1$ data points of the joint trajectory, which divide the moving trajectory of each joint into m sections. According to actual conditions, the optimized target function is given:

$$T = \sum_{j=1}^{m} \Delta t_j = \sum_{j=1}^{m} (t_j - t_{j-1}) \tag{10}$$

where T refers to the total moving time of the arm, and Δt_j stands for the time spent on the jth section of the moving trajectory.

(2) Constraint Condition

During the multi-target trajectory planning of the space robotic arm, the limit conditions of the arm's joint displacement, speed, acceleration and joint force torque are considered as the constraint conditions:

$$\begin{cases} q_j(t) \le \Theta \\ \dot{q}_j(t) \le \dot{\Theta} \\ \ddot{q}_j(t) \le \ddot{\Theta} \end{cases} \tag{11}$$

where $q_j(t)$, $\dot{q}_j(t)$ and $\ddot{q}_j(t)$ stands for the displacement, speed and acceleration respectively in the jth (j=1,2,…..,m) section of the moving trajectory. Θ, $\dot{\Theta}$ and $\ddot{\Theta}$ represents the available maximum displacement, speed and acceleration respectively.

IOP Conf. Series: Materials Science and Engineering **439** (2018) 032077 doi:10.1088/1757-899X/439/3/032077

5. Solutions by Genetic Algorithm

5.1. Optimization

The research target hereof is the 9-degree-of-freedom redundant space robotic arm which has 2 sliding pairs and 7 revolute pairs. The assembly is completed by assembling the sub-mirror modules layer by layer, and the stretchable arm is designed to extend the workspace of the robotic arm, so in the assembling process, the sliding pairs of the arm can be fixed, which means completing the assembling tasks by a 7-degree-of-freedom robotic arm.

In the previous chapter, the arm's joint trajectory is constructed through the cubic B-spline curves, and the control vertex of each joint trajectory is worked out with the given joint trajectory data points during the assembly to determine all constraint conditions for trajectory planning. Take the assembly of the first-layer sub-mirror module as an example, and the joint trajectory data points of the space robotic arm when completing the assembling task are shown in Table 2.

Table 2 Data Points of Joints of the Robotic Arm

data pint (º)	Joint 1	Joint 2	Joint 3	Joint 4	Joint 5	Joint 6	Joint 7
t_0	0	90	0	-180	-180	-90	0
t_1	0	90	-15	-10	-170	-90	0
t_2	0	90	-5	70	-155	-90	0
t3	0	90	-90	0	90	-90	0
t_4	0	90	-135	-60	105	-90	0

In fact, when the arm is performing the assembly task, trajectory planning is not necessary for every joint. The revolving angle of four joints is very small compared with that of their previous joints and they don't take much time, but another three joints have a large revolving angle and take much time, so when making analysis, we can fix Joint 1, 2, 6 and 7, and only conduct time optimal trajectory planning for Joint 3, 4 and 5 which consume longer time.

5.2. Genetic Algorithm Design and Analysis of Optimization Result

The genetic algorithm is used herein to work out solutions for the time-optimal trajectory plan for the space robotic arm, with arm's moving time on each section of the trajectory as the decision variable. Each decision variable is independent from each other and not influenced by each other. Also, with displacement, speed and acceleration of every joint of the arm are set as the constraint conditions, the minimum total moving time as the optimization target, the operating parameters of the genetic algorithm is designed.

With the population size N set at 50, the competition scale St at 2, crossover probability at 0.8, mutation probability at 0.1 and the maximum evolutionary generation T at 100, the optimization process and optimization result of the genetic algorithm are shown in Fig. 9, Fig. 10 and Fig. 11

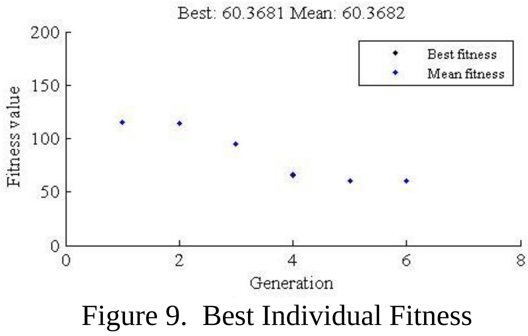

Figure 9. Best Individual Fitness

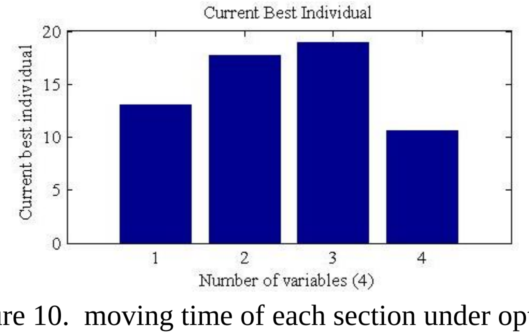

Figure 10. moving time of each section under optimal time

IOP Conf. Series: Materials Science and Engineering **439** (2018) 032077 doi:10.1088/1757-899X/439/3/032077

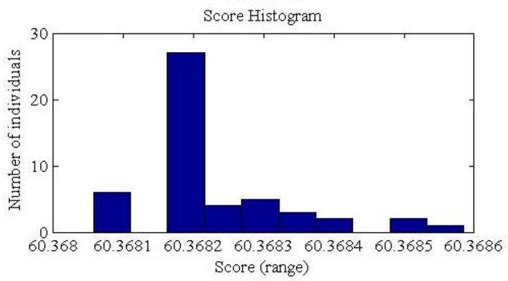

Figure 11. post-optimization range of changes of individual fitness

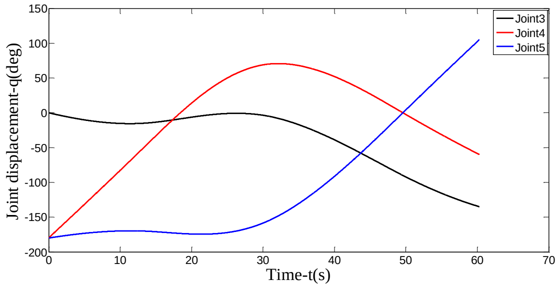

Figure 12. displacement of the robotic arm

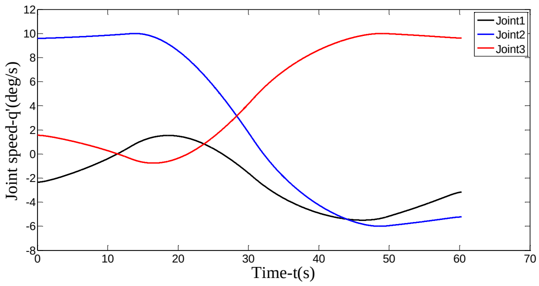

Figure 13. speed of the robotic arm

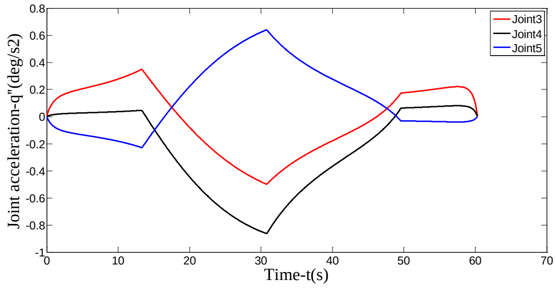

Figure 14. acceleration of the robotic arm

Fig. 9 shows the functional relation between best individual fitness and the evolution generations: as the population evolves, the best individual fitness declines and at last remains stable around the optimal value. Fig. 10 displays the moving time of the each section of the trajectory when the target function reaches the optimal value; Fig. 11 presents the range of individual fitness when it evolves to the last generation, which shows that the fitness of all individuals in the population almost remains at the same level when the population evolves to the last generation, and that's when the target function gets the optimal solution.

Based on the results above, the displacement, speed and acceleration of the three joints of the arm during the moving process are worked out.

6. Conclusion

(1) The space robotic arm can extend the workspace by stretching the arm to deliver all the sub-mirror modules of the telescope to the pre-assembly positions, thus meeting the requirements for the assembly task.

(2) With the uniform cubic B-spline curves, the joint space trajectory of the robotic arm with continuous speed and acceleration can be worked out and the calculation is highly efficient.

(3) Application of genetic algorithm in time-optimal space robotic arm trajectory planning can achieve the minimum moving time of the robotic arm, and the displacement, speed and acceleration of every joint of the arm remain in the safety range, with no risk of mutation, so it is a safe and reliable solution in engineering practice.

Acknowledgments

This work was supported by Postdoctor Scientific Research Foundation for Heilongjiang Province and Harbin Research Fund Technological Innovation(2015RAQXJ015).

References

[1] Quigley M, Asbeck A, Ng A. A low-cost compliant 7-DOF robotic manipulator[C]// IEEE International Conference on Robotics and Automation. IEEE, 2012:6051-6058.

[2] Chettibi T, Lemoine P. Generation of Point to Point Trajectories for Robotic Manipulators Under Electro-Mechanical Constraints[J]. International Review of Mechanical Engineering, IREME, ISSN 1970-8734, 2007, 1(2).
[3] Yang J, Wang H, Chen W, et al. Time-jerk optimal trajectory planning for robotic manipulators[C]// IEEE International Conference on Robotics and Biomimetics. IEEE, 2013:2257-2262.
[4] Das S, Suganthan P N. Differential Evolution: A Survey of the State-of-the-Art[J]. IEEE Transactions on Evolutionary Computation, 2011, 15(1):4-31.
[5] Shi Fazong. Computer aided geometric design and non-uniform rational B spline [M]. Higher Education Press, 2013.